A Fast-Fading Mobile Channel Measurement System

Robert T. Johnk [#1], Chriss A. Hammerschmidt[#2], Mark A. McFarland[#3] John J. Lemmon[#4]

[#]*Institute for Telecommunication Sciences (NTIA/ITS)*
325 Broadway
Boulder, Colorado 80305 USA
[1] bjohnk@its.bldrdoc.gov
[2] chammerschmidt@its.bldrdoc.gov
[3] mmcfarland@its.bldrdoc.gov
[4] jlemmon@its.bldrdoc.gov

Abstract—**We describe a prototype propagation measurement system based on a combination of a spectrum analyzer and a vector signal analyzer. The system is designed to measure the characteristics of a narrowband mobile radio channel. We present results from a commercially-available fading simulator and fixed-to-mobile measurements performed in Boulder, Colorado. The results obtained look promising and the system demonstrates excellent measurement fidelity.**

I. Introduction

The burgeoning wireless revolution and the need for higher efficiency in the use of radio spectrum have spurred much interest in the study of radio-frequency (RF) propagation in the mobile channel. A thorough understanding of propagation is a prerequisite for the successful and efficient operation of mobile radio systems.

Engineers at the Institute for Telecommunication Sciences (NTIA/ITS) are developing a new measurement system to investigate the mobile radio channel. This system is designed to evaluate the fading characteristics of a narrowband mobile radio channel.

The measurement system consists of two primary parts: a transmitter and a receiver. It transmits a continuous-wave (CW) signal from a fixed location to a mobile receiving system located on a van. The van is driven through selected environments and the received signal is routed to both a spectrum analyzer and vector signal analyzer. The spectrum analyzer has two purposes. First, it functions as a real-time signal monitor to continuously observe the levels of the received signal. Second, the spectrum analyzer has a built-in global positioning system (GPS) which enables accurate position tracking. The vector signal analyzer (VSA) is the primary data acquisition system, and it digitizes the received signal and down-converts it to a discrete time series of baseband in-phase (I) and quadrature (Q) components. We post-process the resulting complex time series signal to analyze selected channel characteristics.

We performed a two-part evaluation of this system. First, we used a mobile-radio channel simulator to mimic the effects of a CW signal transmitted through a Rayleigh channel. The channel simulator is used for testing the performance of commercial digital and analog mobile radios for a wide variety of user-selected fading conditions. We applied the simulator signal to the receiver section and recorded a 600 second time series of the baseband I-Q samples using the VSA. We simulated a non-line-of-sight (NLOS) Rayleigh channel with a receiver moving at a constant velocity.

The second part of this effort consisted of actual fixed-to-mobile measurements. We located the transmitting antenna on the roof of Building 1 at the Department of Commerce Laboratories in Boulder, CO (Commerce labs). We installed the receiving system in a custom-designed van. We drove the van in a prescribed pattern through residential neighborhoods adjacent to the labs. The drive route was designed to provide both line-of-sight (LOS) and non-line-of-sight conditions.

The results show much promise and indicate that this measurement system is a useful tool.

II. Measurement System

A schematic diagram of the mobile measurement system is shown in Fig. 1. The transmitter consists of a frequency synthesizer, rubidium clock, RF power amplifier, low-pass filter, and a transmitting antenna. We program the synthesizer to generate a 430 MHz, CW sinusoidal signal at a power level of -5 dBm. The frequency synthesizer is disciplined using a 10 MHz rubidium frequency reference, with a nominal accuracy of one part in 10^{12}. It provides a stable and precise transmitted frequency that is required for propagation measurements. The power amplifier boosts the signal to +40 dBm (10 W) at the transmitting antenna port. The transmitting antenna, shown in Fig. 2(a), is located on the roof of Building 1, on the campus of the Commerce labs. The antenna is a stacked coaxial array, located inside a protective plastic radome. It has an omnidirectional azimuthal pattern and a gain of 5 dBi.

The receiving system consists of a monopole antenna, two-way power splitter, VSA, and a spectrum analyzer. A 10 MHz rubidium clock is used to discipline the spectrum analyzer and VSA. The receiving equipment is installed in the specially-designed van shown in Fig. 2(b). This van was earlier used to perform wideband channel measurements [1]. It has a custom-built aluminum ground plane for the installation of antennas and to provide stable and controlled patterns. It has equipment racks and a 5 kW generator to power the equipment.

- Certain commercial equipment and materials are identified in this paper to specify adequately the technical aspects of the reported results. In no case does such identification imply recommendations of endorsement by the National Telecommunications and Information Administration, nor does it imply that the material or equipment is the best available for this purpose.

978-1-4673-2060-3/12/$31.00 ©2012 IEEE

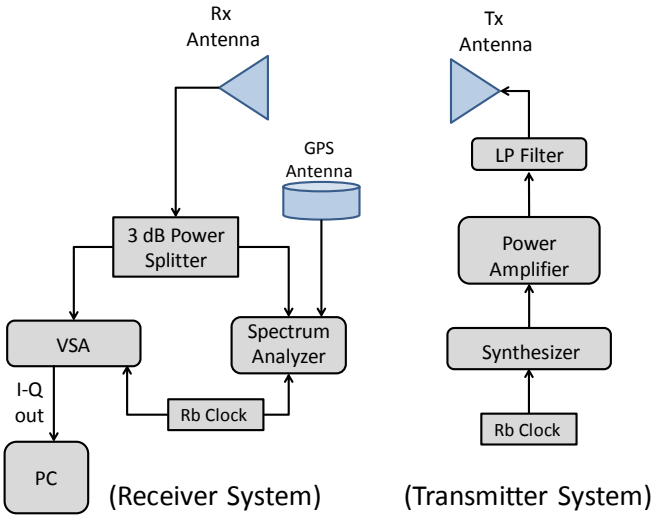

Fig. 1. Fixed-to-mobile propagation measurement system schematic.

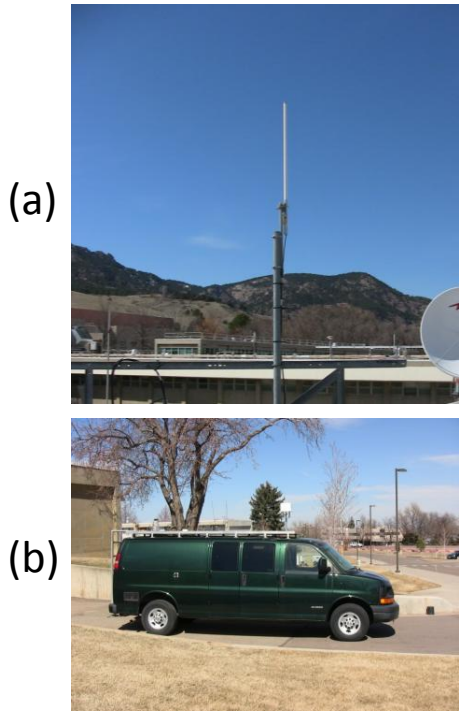

Fig. 2. a. Transmitter antenna at the Boulder labs. b. The receiver van.

The VSA uses a high-speed digitizer and digital signal processing (DSP) to acquire the signal and down-convert it to a complex time series at baseband. The time series contains I and Q samples. The I-Q time series is the starting point and basis for our propagation analysis. The ability to create complex I-Q samples is a powerful feature for propagation studies.

One drawback of the VSA is that it does not allow the received signal to be monitored in real time while it is recording data. The spectrum analyzer enables us to monitor the received signal in real time. This ensures that we are neither experiencing on-channel overloading of the system nor encountering environmental interference.

The spectrum analyzer also has a built-in GPS receiver which enables us to determine the position at which the data are taken. The GPS has an x-y positional accuracy of 2.5 m, and it updates at a rate of once per second. The analyzer stores the GPS time and positional coordinates which are later transferred to a computer for subsequent post-processing.

We also developed a test setup, shown in Fig. 3, based on a commercially available fading simulator. We applied the fading simulator output to the receiving system at the antenna input connector. We configured the simulator to produce a Rayleigh-faded signal to test our receiving system and validate our post-processing software and algorithms.

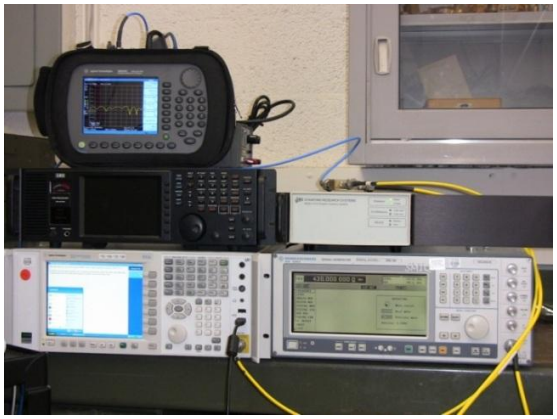

Fig. 3. The fading simulator feeding the vector signal analyzer/spectrum analyzer combination. The fading simulator is located on the bottom right, and VSA and spectrum analyzer are located on the top and bottom left respectively. The rubidium clock is sitting at the top right.

III. CHANNEL PARAMETERS

A vector signal analyzer is the primary data acquisition component, and it digitizes the received signal and down-converts it to a discrete time series of baseband in-phase and quadrature components. We post-process the resulting complex time series signal to analyze selected channel characteristics. We are primarily interested in the following statistical channel parameters:

- Probability density function (pdf) of the signal envelope
- Autocovariance function of the signal envelope
- Power spectral density of the signal envelope
- Autocovariance of the in-phase (I) component
- Power spectral density of the in-phase (I) component

For the purpose of initial validations, we did not investigate the channel phase characteristics. The channel parameters provide insight into the propagation characteristics of the channel, and they are useful for facilitating the design and successful operation of land-mobile radio systems.

The post-processing sequence is shown in Fig. 4. The output of the VSA is stored as discrete time series of complex I-Q samples, $s(t_n)$, where $(n=1,2,\ldots)$. We choose an interval of interest of the recorded time series and estimate selected first-

and second-order statistical metrics. The processing consists of two main paths. In the first path, we process the signal envelope $|s(t_n)|$; in the second, parallel path, we process the in-phase component $I(t_n)$. The first processing step, in either path, is to divide each signal sample by a running average of data points

$$f_d(t_n) = \frac{f(t_n)}{\sum_{n-\frac{W}{2}}^{n+\frac{W}{2}} f(t_n)}$$

where f denotes the time series and W denotes a window width that is symmetrically placed about the point t_n. This process is called demeaning [2], and it removes the effects of slow fading and extends the interval over which the time series is stationary [2]–[4]. Once we demean the signal envelope, we use the probability distribution tool in MATLAB® to obtain a maximum likelihood estimate of the first-order channel pdf.

The second-order statistical analysis is the same for both the envelope and the I-component. The next step is to compute the autocovariance of a selected interval of the demeaned time series. This function is also computed using routines available in MATLAB. Since we are measuring a random process, we need to apply a properly conditioned spectral estimation technique to the time series. We chose Welch's method [5]–[7] because it is straightforward to apply to the selected time series. It yields accurate and stable results. We implement this by first subdividing the time series into equal-length segments. We then apply a fast Fourier transform to each individual segment and average the results to estimate the power spectral density.

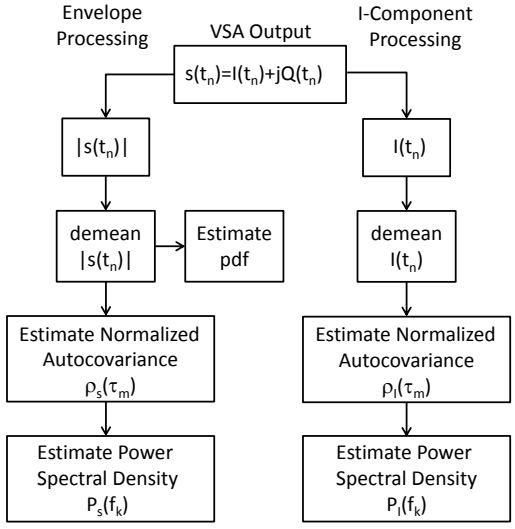

Fig. 4. Signal processing for the estimation of parameters.

IV. CHANNEL SIMULATOR AND FIXED-TO-MOBILE TESTS

We performed a series of tests of our measurement system using the setup diagrammed in Fig. 5. The fading simulator generates an RF signal with a sophisticated combination of amplitude, frequency, and phase modulations to emulate a fading channel. We configured it to simulate travel through a NLOS Rayleigh channel at a constant velocity. We also programmed it for a Jakes power spectral density [8].

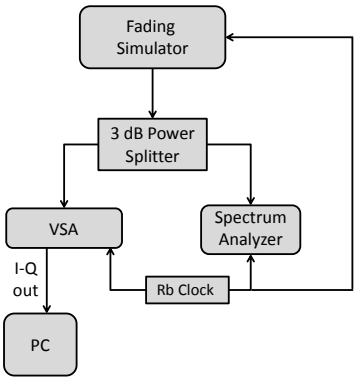

Fig. 5. Configuration for the fading simulator tests.

For the simulator tests, we set the frequency at 430 MHz and fed the signal to the receiving system. We performed a series of tests with simulated van velocities in the range of 5–30 mph (2.46–14.76 m/sec). We set the VSA bandwidth to 1 kHz and recorded I-Q samples at a sampling rate of 1,285 Hz, capturing more than 90 samples per wavelength at a speed of 20 mph (9.84 m/sec). This sampling rate ensured that the channel was well oversampled with high measurement fidelity.

We performed a series of fixed-to-mobile tests in which we transmitted a 430 MHz CW signal from our laboratory to a mobile receiving van. We drove our receiving van through residential neighborhoods adjacent to the Commerce labs. We successfully maintained a constant speed of 20 mph throughout most of the drives. Fig. 6 depicts the typical residential area that was encountered during the drive. The residential neighborhoods consist primarily of single-story houses on quarter-acre lots with plenty of trees and shrubs. The drive route had segments that were in direct line-of-sight of our transmitting antennas, as well as segments that were completely non-line-of-sight. The GPS coordinates and time were captured and recorded by the spectrum analyzer, and were later used for geolocation of the measured VSA data. The range of transmitter/receiver separations was 0.5–3.5 km.

Fig. 6. A typical residential neighborhood that was encountered during the drive tests.

V. Results and Intercomparisons

Figs. 7(a)–(c) show 10 second long VSA envelopes obtained from the fading simulator set for 20 mph, a NLOS Rayleigh drive route segment, and a LOS drive segment. The received envelopes show rapid variations due to fast fading. We also plot the running averages for W=1 s. The results obtained from the simulator and the NLOS drive tests are strikingly similar in character. The LOS results have a much different character and have a visible deterministic component that is due to the presence of a direct path. We performed the same analysis for W=2, 3, 4 seconds as well. The longer window produced small changes in the first- and second-order statistics.

The first-order statistics are shown in Figs. 8(a)–(c). The demeaned signal envelope sample amplitudes are used to construct histograms and estimate the channel pdfs. Once again, the simulator and NLOS drive tests exhibit similar behavior. The estimated channel pdfs are nearly the same and are Rayleigh. In the LOS case, the distribution is quite different and is shifted due to the direct path component. The estimated channel pdf is Rician.

The I-component covariances are shown in Figs. 9(a)–(c). As a benchmark, we also plot the analytical results for the autcovariance of a Jakes channel [8]. The simulator and NLOS results closely agree with theory. The behavior of the LOS results is much different from that of the NLOS results, as expected.

The corresponding power spectral density estimates are shown in Figs. 10(a)–(c). The simulator and NLOS drive segment results agree well and the sharp peaking in the spectrum corresponds to the expected Doppler shift of 12.8 Hz at 20 mph. We have not plotted the theoretical Jakes result because our estimated power spectral densities are relative, not absolute, and differ from theory by an unknown, multiplicative constant. However, the resulting power spectral densities do have a shape quite similar to that of the Jakes model. The LOS case shows a much stronger, almost impulsive, behavior at 12.8 Hz. This was caused by the combination of the van moving away from the transmitter at 20 mph and a dominant direct path component.

The envelope autocovariance results are plotted in Figs. 11(a)–(c). Once again, we provide comparisons with a theoretical Jakes channel [8]. The envelope autocovariances obtained for the simulator and the NLOS cases do not exhibit the good agreement after the central lobe that we saw with the I-channel results. As will be seen shortly, this is due to slower convergence of the envelope estimates. The LOS case departs significantly once again due to the direct path component, and exhibits Rician behavior.

The envelope power spectral densities are plotted in Figs. 12(a)–(c). The shapes of the power spectral densities are similar to those reported in Parsons [4]. The power spectral densities show strong peaking at 0 Hz. and drop off rapidly above 25.6 Hz—an artifact of the nonlinear envelope operation.

In order to investigate the convergence issues, we computed autocovariance and associated power spectral densities for increasing record lengths using the fading simulator. Figs. 13(a)–(b) and Figs. 14(a)–(b) show the autocovariances and power spectral densities for a 200 second long VSA record. The I-channel autocovariance results agree even better and almost overlay. Good agreement is seen in the corresponding envelope results. The I-channel power spectral density is much cleaner and more sharply peaked at the 20 mph Doppler shift. The resulting envelope power spectral density is less noisy and better defined. The differences in rates of convergence for the envelope and I-component autocovariances are a bit of surprise, and we will need to conduct a statistical analysis to better understand this phenomenon. We should also note that while a 200 second time series can be easily generated and measured using a simulator, it simply is not practical to process records of that length in fixed-to-mobile scenarios. Environmental considerations impose a limit of approximately 15–20 seconds before the channel stationarity assumption is no longer valid.

VI. Conclusions

ITS engineers have developed and tested a mobile propagation measurement system that is based on a combination of a VSA and a spectrum analyzer with a built-in GPS receiver. The system has been used for narrowband fast-fading measurements, and good measurement fidelity has been achieved. We evaluated the system using a combination of a fast-fading simulator and fixed-to-mobile measurements. The results show much promise, and in some cases excellent agreement with theoretical models can be achieved. More tests are planned to further study this system.

Acknowledgment

The authors thank Dr. Roger Dalke of the Institute of Telecommunication Sciences (NTIA/ITS) for many useful discussions on radio propagation. The authors would also like to thank John Ewan of NTIA/ITS for his insights and assistance on instrumentation issues.

References

[1] R.T. Johnk, P. Papazian, P. McKenna, N. DeMinco, G. Sanders, H. Ottke, "A mobile propagation measurement system," *IEEE International Symposium on EMC,* August 2009, pp. 103-108.

[2] R. Vaughan and J. B. Andersen, *Channels Propagation and Antennas for Mobile Communications,* The Institution of Electrical Engineers, London, U.K, 2003.

[3] R.H. Clark, "A statistical theory of mobile radio reception," *Bell System Technical Journal,* Vol. 47, Issue 6, July-August 1968.

[4] J.D. Parsons, *The Mobile Radio Propagation Channel,* New York, NY, John Wiley & Sons, 1992.

[5] R. Shiavi, *Applied Statistical Signal Analysis,* Burlington, MA, Elsevier, 2007.

[6] S. M. Kay, *Modern Spectral Estimation,* Upper Saddle River, N.J., Prentice-Hall, 1987.

[7] A.V. Oppenheim and R.W. Shafer, *Discrete-Time Signal Processing,* Upper Saddle River, N.J., Prentice-Hall, 2010.

[8] A.F. Molisch, *Wireless Communications,* New York, NY, John Wiley & Sons, 2010.

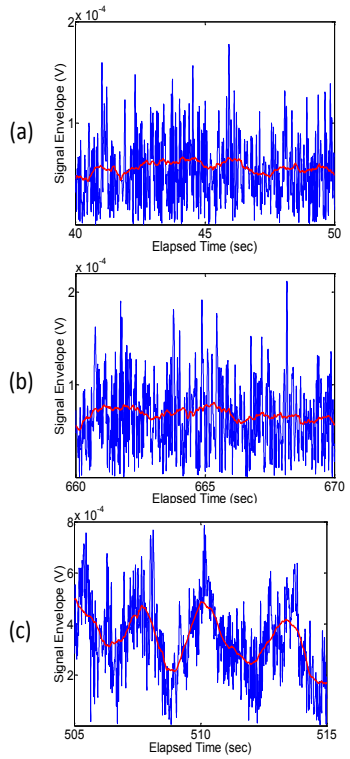

Fig. 7. Received signal envelopes (blue) and running means (red) with W=1 sec (red): (a) channel simulator configured for a Rayleigh-faded Jakes channel, (b) measured NLOS signal, and (c) measured LOS signal.

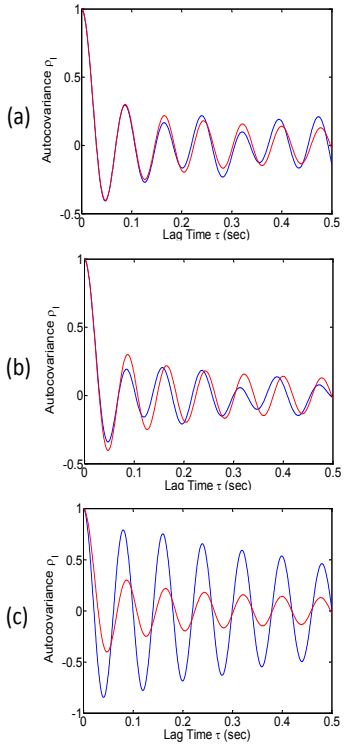

Fig. 9. Measured I-component autocovariances from a 10-second record (blue) and a theoretical Jakes channel calculation (red): (a) channel simulator, (b) measured NLOS Rayleigh channel, (c) measured Rician LOS channel.

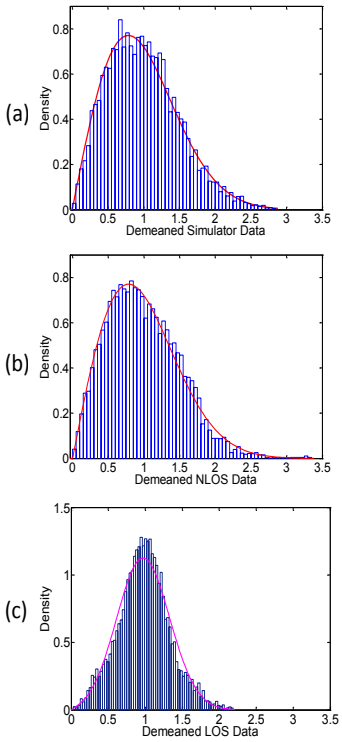

Fig. 8. Envelope histograms (blue) and estimated pdf fits (red) based on a 10-sec record for (a) channel simulator, (b) NLOS Rayleigh-faded channel measurement, and (c) LOS Rician channel. The abscissa has the units of normalized volts.

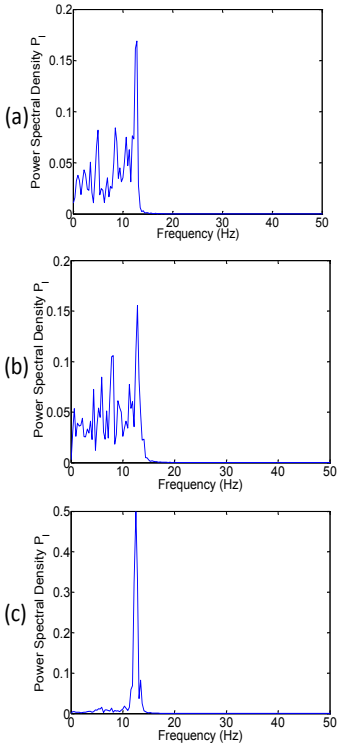

Fig. 10. Welch I-component power spectral density (W/Hz) for (a) channel simulator, (b) NLOS Rayleigh-faded channel, and (c) LOS Rician channel.

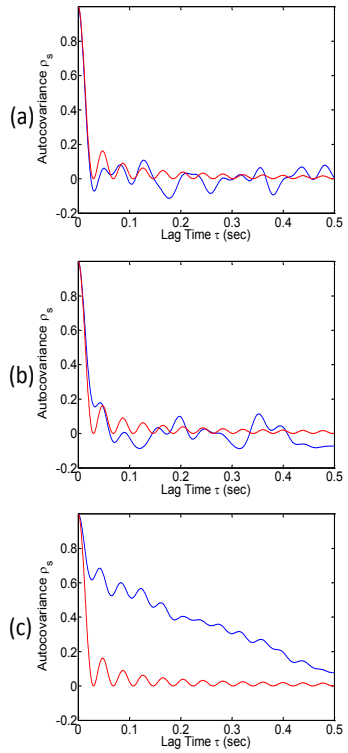

Fig. 11. Measured envelope autocovariances from a 10-second record (blue) and a theoretical Jakes channel calculation (red): (a) channel simulator, (b) measured NLOS Rayleigh channel, (c) measured Rician LOS channel.

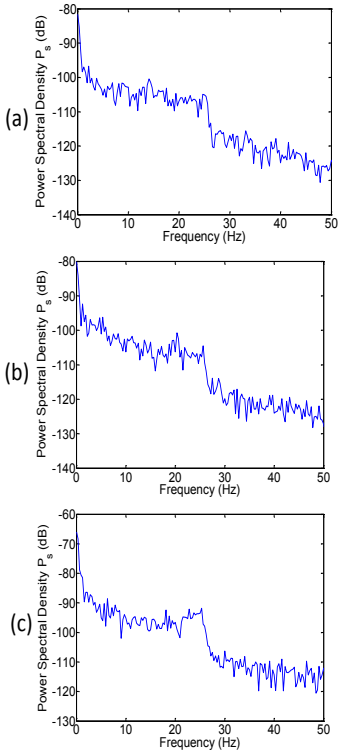

Fig. 12 Welch envelops power spectral densities (dBW/Hz) for (a) channel simulator, (b) NLOS Rayleigh-faded channel, and (c) LOS Rician channel.

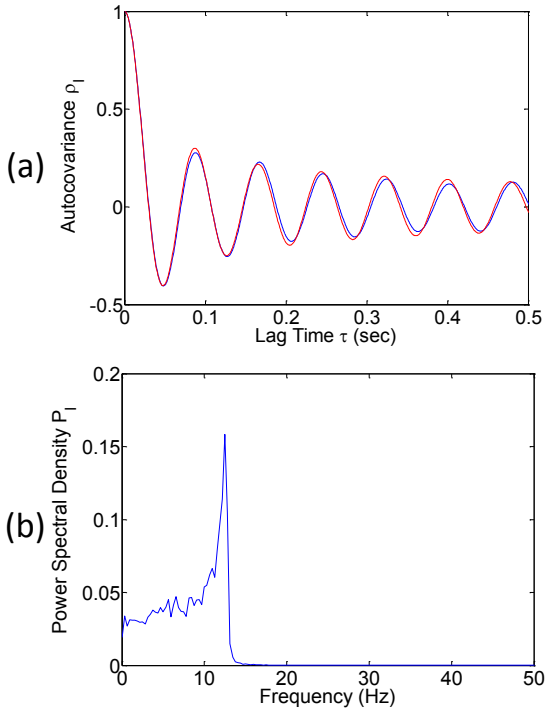

Fig. 13. (a) Comparison of measured I-component autocovariances from a measured 200-second channel simulator record (blue) and a theoretical Jakes channel (red). (b) Measured channel simulator I-component power spectral density (W/Hz).

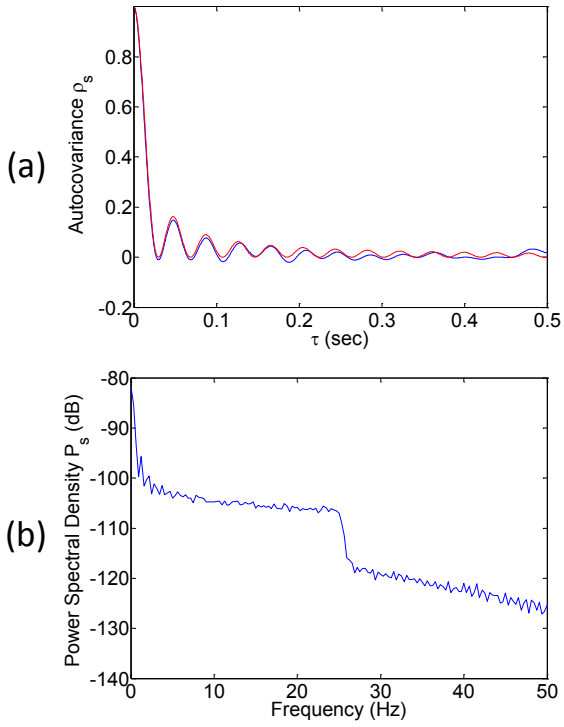

Fig. 14. (a) Comparison of measured envelope autocovariance (blue) from a measured 200-second channel simulator record and a theoretical Jakes channel (red). (b) Welch channel simulator envelope power spectral density (dBW/Hz).